Title

Neural basis of the visual working memory deficit in schizophrenia: Merging evidence from fMRI and EEG

Authors

Erickson, Molly A
Hahn, Britta
Kiat, John E
et al.

Publication Date

2021-10-01

DOI

10.1016/j.schres.2021.07.039

Peer reviewed

HHS Public Access

Author manuscript

Schizophr Res. Author manuscript; available in PMC 2022 October 01.

Published in final edited form as:

Schizophr Res. 2021 October ; 236: 61–68. doi:10.1016/j.schres.2021.07.039.

Neural basis of the visual working memory deficit in schizophrenia: merging evidence from fMRI and EEG

Molly A. Erickson[1,a], **Britta Hahn**[2], **John E. Kiat**[3], **Luz Maria Alliende**[1], **Steven J. Luck**[3], **James M. Gold**[2]

[1]Department of Psychiatry & Behavioral Neuroscience, University of Chicago, 5841 S. Maryland Ave, Chicago, IL 60622

[2]Maryland Psychiatric Research Center, University of Maryland School of Medicine

[3]Center for Mind & Brain and Department of Psychology, University of California, Davis

Abstract

Although people with schizophrenia (PSZ) exhibit robust and reliable deficits in working memory (WM) capacity, the neural processes that give rise to this impairment remain poorly understood. One reason for this lack of clarity is that most studies employ a single neural recording modality—each with strengths and weaknesses—with few examples of integrating results across modalities. To address this gap, we conducted a secondary analysis that combined data from an overlapping set of subjects in previously published electroencephalographic and functional magnetic resonance imaging studies that used nearly identical working memory tasks (visual change detection). The prior studies found similar patterns of results for both posterior parietal BOLD activation and suppression of the alpha frequency band within the EEG. Specifically, both signals exhibited abnormally shallow modulation as a function of the amount of information being stored in WM in PSZ. In the present study, both alpha suppression and posterior parietal BOLD activity increased as the number of items stored in WM increased. The magnitude of alpha suppression modulation was correlated with the magnitude of BOLD signal modulation in PSZ, but not in HCS. This finding suggests that the same illness-related biological processes constrain both alpha suppression and BOLD signal modulation as a function of WM storage in PSZ. The complementary strengths of these two techniques may thus combine to advance the identification of the processes underlying WM deficits in PSZ.

[a]Corresponding author merickson1@uchicago.edu.

Contributors

The idea for the manuscript was originally developed by Drs. Erickson and Hahn, who wrote the first draft of the paper. Dr. Kiat conducted statistical analyses for the manuscript. All other authors contributed to the subsequent manuscript drafts.

Disclosures

The authors have no conflicts of interest to report.

Keywords

EEG; fMRI; visual working memory; schizophrenia; alpha oscillations; event-related desynchronization; posterior parietal cortex

Introduction

Working memory (WM) is a cognitive domain that is robustly impaired among people with schizophrenia (Johnson et al., 2013; Lee and Park, 2005), although its biological underpinnings remain poorly understood. A large number of investigations have attempted to pinpoint the primary impairment that produces the WM deficit in PSZ, but these efforts have been frustrated by (a) the wide variety of WM tasks in use, and (b) the varied methodologies used to measure brain activity, each with its own strengths and weaknesses. As a result, the number of potential mechanisms are nearly as varied as the methods used to study WM in PSZ.

Within the functional magnetic resonance imaging (fMRI) literature on WM in PSZ, this heterogeneity has been largely due to differences in WM tasks. WM paradigms that challenge executive control by requiring manipulation or active updating of the encoded items have produced abnormal activation patterns in the prefrontal cortex of PSZ (Glahn et al., 2005; Kraguljac et al., 2013; Manoach, 2003; Snellenberg et al., 2006). By contrast, tasks that engage WM storage *without* emphasizing executive control have revealed abnormalities in posterior parietal cortex (PPC) activation (Hahn et al., 2018, 2017). In these studies, the pattern of abnormalities in PSZ consists of hypoactivation relative to healthy control subjects (HCS) when WM load is high, and hyperactivation when WM load is low. Consequently, PSZ exhibit a significantly shallower BOLD signal increase in these areas as a function of WM load (Hahn et al., 2018). These observations provide important clues about the functional role of neuroanatomical structures in the WM deficit in PSZ. However, due to the limitations of the BOLD signal—namely, its slow temporal dynamics and its indirect measurement of neural activity—conceptual gaps remain that may be bridged using converging evidence from methods designed to capture rapid neural processes such as electroencephalography (EEG).

Unlike fMRI, EEG is advantageous for directly measuring neural oscillatory processes that can become disrupted during WM in PSZ. For instance, we and others have observed abnormally reduced event-related suppression of the alpha frequency band (9-12 Hz) in posterior cortical regions that emerges shortly after the onset of an array of to-be-remembered stimuli in PSZ (Bachman et al., 2008; Erickson et al., 2017; Kang et al., 2018). In neurotypical individuals, posterior alpha suppression is consistently (a) more pronounced with more items maintained in WM, and (b) associated with individual differences in WM capacity (Erickson et al., 2019; Fukuda et al., 2015). We have found that, in addition to an overall reduction in alpha suppression, PSZ exhibit significantly shallower increases in alpha suppression as a function of WM load (Erickson et al., 2017), mirroring the pattern of PPC BOLD impairment described above (Hahn et al., 2018). The pattern similarities between the two indices suggest that they may be constrained by a common structural or functional

impairment. To date, however, it remains unclear whether alpha suppression and BOLD abnormalities reflect the same pathology in neuronal function underlying WM deficits in PSZ.

The purpose of the present study was to address this unanswered question by conducting a secondary analysis of EEG (Erickson et al., 2017) and fMRI (Hahn et al., 2018) data from nearly identical visual WM tasks, collected from partially overlapping samples of HCS and PSZ. We then examined the correlation between PPC BOLD and posterior alpha suppression modulation from participants who completed both protocols. We predicted that the magnitude of signal modulation as a function of WM storage would be associated with one another; such an observation would constitute preliminary evidence that the two indices reflect a common neural mechanism of WM impairment, and would be a first step toward integrating neuroimaging markers of WM deficits in PSZ and associated pathological network processes.

Methods

Participants

Of the 30 PSZ and 31 HCS who completed the EEG task and the 37 PSZ and 37 HCS who completed the fMRI task, 18 PSZ and 22 HCS completed both paradigms and were included in the present study (see Table 1). There were no differences in sample characteristics between participants who completed both paradigms compared to those who completed only one (see Supplementary Table 1). PSZ and HCS were similar in age, both when performing the EEG paradigm and when performing the fMRI paradigm, as well as in gender, race, and parental education, a proxy measure for socioeconomic status. The two groups differed in IQ and education level. PSZ did not differ in symptom severity, social and occupational functioning, or medication dose between the EEG and the fMRI testing session, which were on average 3 months apart. 13 PSZ and 13 HCS completed the EEG testing session first, and 5 PSZ and 7 HCS completed the MRI testing session first. See Supplement for medications at time of testing.

Inclusion criteria for PSZ were (a) a DSM-IV-TR (First et al., 2002) diagnosis of schizophrenia or schizoaffective disorder; and (b) psychiatric stability with no changes in medication for at least 4 weeks before testing. Inclusion criteria for HCS were (a) no current Axis I diagnosis; (b) no history of psychosis or schizotypal personality disorder; (c) not currently taking psychiatric medications; and (d) no family history of psychosis. Both groups of participants were 18-55 years old, reported no history of neurologic injury, and had normal or corrected-to-normal vision established using a Snellen eye chart and the Ishihara test for colorblindness. All procedures were approved by the University of Maryland Institutional Review Board. Written informed consent was obtained from all participants.

Experimental Task

In both studies, participants completed a change detection paradigm (Luck and Vogel, 1997) with minor differences between the two tasks. In the EEG study, participants viewed stimuli

on an LCD monitor with a gray background and a continuously visible central fixation cross at a viewing distance of 100 cm while EEG was recorded. On each trial, a sample array was presented for 200 ms containing 1, 2, 4, or 6 colored squares (Figure 1 A) arranged around an invisible circle with a radius of 4.1° visual angle. The colors of the squares were drawn randomly without replacement from the following list: red, white, black, blue, purple, green, and yellow. Following the offset of a sample array was an 1800-ms delay interval during which participants retained the colors of the squares in memory. At the end of the interval, a test array was presented in which all squares from the sample array reappeared. On 50% of trials, all of the colors remained the same; on the other 50% of trials, one of the squares changed to a new color. Participants indicated by button-press response whether the test array was the same as or different from the sample array. Participants completed 96 trials of each set size.

The task parameters of the fMRI study were identical with the following exceptions (Figure 1B): stimuli were presented on a black background, and the list of possible colors included: red, magenta, purple, blue, teal, cyan, green, olive, yellow, and white. Following the offset of the 200-ms sample array, the delay period ranged from 1100-4400 ms before a test array appeared, probing recall for one of the sample array items. Again, the probability that the test item changed color was 50%, and participants indicated whether the item was the same or different from the sample array color. Given that the precision of these WM representations appears to remain stable over a period of at least 4000 ms in both PSZ and HCS (Gold et al., 2010), as well as the fact that participants did not have advance knowledge about which item from the sample array would be probed at test in the fMRI task, we consider these task differences to be of minor impact on the brain processes described here (but see Discussion for additional considerations). Finally, in the fMRI version, set size 7 was also included; data from these trials were eliminated from the present analysis. Participants completed 40 trials of each set size.

We computed an estimate of the number of items stored in WM for each subject at each set size, which is denoted *K*. As the fMRI task was a partial-report design, K in this paradigm was calculated as (hit rate – false alarm rate) * set size (Cowan, 2001). The EEG task used a full-report design, and K from this paradigm was thus calculated as ((hit rate – false alarm rate)/(1-false alarm rate) * set size) (Pashler, 1988; Rouder et al., 2011). Of note, *K* at set size 4 is considered the closest estimate of WM capacity because it is least limited by ceiling effects or by selection demands at large set sizes. No order effects on task performance were observed (see Supplement).

EEG recording, preprocessing, and signal measurement

Details of the EEG methods are described by Erickson et al. (2017) Briefly, the EEG was continuously recorded from 32 scalp locations using a BioSemi ActiveTwo EEG recording system (BioSemi B.V., Amsterdam, Netherlands). Data were low-pass filtered online with a half-power cutoff at 208 Hz and digitized at 1024 Hz. Vertical and horizontal electrooculograms were also recorded.

All offline data processing was conducted in Matlab (The MathWorks, Inc., Natick, MA) using EEGLAB (Delorme and Makeig, 2004) and ERPLAB (Lopez-Calderon and Luck,

2014) toolboxes. Data were referenced to the average mastoid electrodes and then down sampled to 512 Hz. Data were then segmented into 4-second epochs time-locked to the onset of the sample array, which included a 1500 ms baseline period and a 2500 ms post-stimulus period, and baseline corrected to the mean pre-stimulus voltage. Artifact correction was performed using Independent Components Analysis to remove blinks and eye movements from the data, after which ERPLAB artifact rejection routines and visual inspection were conducted to identify and eliminate remaining artifacts. HCS retained 75% of trials whereas PSZ retained 70% of trials (t_{38}=1.03; p=0.31). No participants retained fewer than 50% of data epochs.

Following pre-processing, time-frequency analysis was conducted on single trials by convolving a Hanning-tapered three-cycle Morlet wavelet with the EEG from each channel using the newtimef.m EEGLab function. Alpha power (9-12 Hz) was measured from 8 posterior electrodes over the left hemisphere (P1, P3, P5, P7, P9, PO3, PO7, and O1) and 8 posterior electrodes over the right hemisphere (P2, P4, P6, P8, P10, PO4, PO8, and O2) from the entire delay period, and transformed to the proportional change in power relative to the 1500 ms baseline period on a logarithmic scale (dB). Electrodes within each hemisphere were then averaged together to calculate left (LH) and right (RH) hemisphere alpha suppression.

Magnetic Resonance Imaging

Details of the fMRI methods are described by Hahn et al. (2018). Briefly, whole-brain EPI images for measuring T2*-weighted BOLD effects [4-mm oblique (13.5°) axial slices, 128x128 matrix, FOV=22x22 cm, TR=2 s, TE=27 ms, FA=90°] were acquired on a 3-Tesla Siemens Tim Trio scanner (Erlangen, Germany). Anatomical reference was obtained from an axial T1-weighted image (0.8-mm^3 voxels, TR=2.2 s, TE=2.83 ms, FA=13°). Data were processed using AFNI (Cox, 1996). Each volume was registered to a base volume. Several control analyses verified that head motion did not differ between HCS and PSZ (Hahn et al., 2018). The time series was analyzed by voxel-wise multiple regression. Regressors corresponding to the five set sizes were expressed as a delta function time-locked to the onset of each encoding array, convolved with a model hemodynamic response function and its derivative. Regressors of no interest corresponded to retrieval array onset, array onsets on trials with no or premature responses, and the six motion parameters. Thus, for each subject, voxel-wise amplitude of signal change produced by each set size was determined. These maps were resampled to a 1-μL resolution, converted to standard space (Talairach and Tournoux, 1988), and spatially blurred (Gaussian 5-mm RMS).

At the group level, whole-brain voxel-wise multiple linear regression was performed on these maps from 74 subjects (the original sample) to define regions whose signal was related to WM storage irrespective of diagnostic group. K was the regressor of interest. Group (HCS, PSZ), the group x K interaction, set size, and subject were included as regressors of no interest. Voxel-wise P<0.001 combined with a 946-μL clustersize threshold yielded overall P<0.05 based on Monte Carlo simulations. Three clusters, described previously (Hahn et al., 2018), displayed greater activation with more items maintained. A right-hemispheric cluster spanned superior and inferior parietal lobule (SPL, IPL) and intraparietal

sulcus (IPS), as well as right middle occipital gyrus (MOG). Symmetrical left PPC and MOG regions were identified in two separate clusters. For the present study, we focus on left and right PPC. Right PPC was manually separated from right MOG along anatomical boundaries (Table 2). Analyses of left and right MOG, the results of which closely adhered to those of the PPC, are presented in the Supplement. For each subject, BOLD activity was averaged within each cluster at each set size.

Statistical analysis

First, we examined whether the subsample of participants from the original studies (a) performed the WM task similarly across the fMRI and EEG testing sessions, and (b) exhibited patterns of alpha suppression and BOLD modulation that mirrored that of the original, full sample. To accomplish this, repeated-measures ANOVAs were conducted on task performance (set size x diagnosis x testing session), PPC BOLD modulation (hemisphere x set size x diagnosis), and alpha suppression (hemisphere x set size x diagnosis).

Second, we examined the relationship between alpha suppression and BOLD signal at each set size and tested the hypothesis that the correlation between these two indices is similar between diagnostic groups. To do this, we used a general linear model with PPC BOLD as the dependent variable and alpha suppression, set size and diagnostic status as fully interacting predictors.

Finally, and of central interest to the study, we examined the correlation between load-dependent alpha suppression and BOLD modulation. To extract a measure of signal modulation as a function of WM load, each participant's BOLD activity and alpha suppression at each set size were paired with K at that set size, and the four BOLD-K or alpha suppression-K pairs were entered into a linear regression model (with K as the predictor and alpha suppression or BOLD as the dependent factor) to obtain the slope of the relationship between K and the respective neuronal activity index for each participant. Due to non-normality of slope distribution, statistical analyses involving slope employed non-parametric tests. Spearman correlation coefficients were calculated to examine the relationship between BOLD slope and alpha suppression slope, as well as their associations with symptom severity, cognitive function, and chlorpromazine equivalents (Andreasen et al., 2010). The same pattern of results was observed using parametric tests.

Results

Behavioral Data

The mean number of items stored in WM at each set size (K) from both experimental sessions is presented in Figures 2A and 2B. As in the full samples, there was a main effect of set size ($F_{3,114}=15.77$; $p<0.001$; $\omega_p^2=0.16$) and group ($F_{1,38}=6.31$; $p<0.05$; $\omega_p^2=0.06$). Importantly, no significant session x set size x diagnosis interaction was observed ($F_{3,114}=0.21$; $p=0.89$; $\omega_p^2=-0.01$), indicating that the pattern of group differences in K across set sizes did not significantly differ between the EEG and fMRI sessions.

Alpha suppression and BOLD signal across set sizes, hemispheres, and diagnostic groups

Figure 3 summarizes the alpha suppression and fMRI results. As in the full samples, alpha suppression increased across set size ($F_{3,114}$=7.84; p<0.001; ω_p^2=0.02) and was reduced in PSZ relative to HCS ($F_{1,38}$=12.57; p=0.001; ω_p^2=0.13). Note that *increases in alpha suppression* are represented by larger negative values as set size increases, and *reduced alpha suppression in PSZ* refers to smaller negative values compared to HCS. Furthermore, there was a significant set size x diagnosis interaction ($F_{3,114}$=3.21; p<0.05; ω_p^2=0.01). Similarly, BOLD increased across set size ($F_{3,114}$=12.32; p<0.001; ω_p^2=0.10), was significantly different across groups ($F_{1,38}$=4.60; p<0.05; ω_p^2=0.04), and exhibited a significant set size x diagnosis interaction ($F_{3,114}$=3.97; p=0.01; ω_p^2 = 0.03). Neither alpha suppression nor BOLD modulation exhibited a significant effect of hemisphere or interaction involving hemisphere (F's<1.11; p's>0.29); as a result, data were averaged over the left and right hemispheres for further analyses.

Relationship between alpha suppression and BOLD

The relationship between alpha suppression and PPC BOLD at each set size, averaged across hemispheres, was assessed using a general linear model with robust standard errors and PPC BOLD as the dependent variable. We observed significant main effects of set size ($F_{3,106}$=34.93; p<0.05; ω_p^2=0.39) and diagnosis ($F_{1,38}$=4.46; p<0.05; ω_p^2=0.02), which were conditionalized by a significant two-way interaction between alpha suppression and set size ($F_{3,106}$=2.72; p<0.05; ω_p^2=0.01) as well as the predicted three-way interaction between alpha suppression, set size and diagnosis ($F_{3,106}$=3.21; p<0.05; ω_p^2=0.04). Follow-up analyses revealed that PSZ had a numerically stronger negative correlation between alpha suppression and BOLD than HCS at all set sizes, with the effect reaching significance at set size 4 (see Figure 4; t_{106}=3.24; p<0.01). That is, larger alpha suppression (i.e., more negative values) was associated with larger BOLD (i.e., more positive values) in PSZ compared to HCS, particularly at set size 4.

Signal modulation with the number of items stored in WM (K)

In neurotypical individuals, both alpha suppression and PPC BOLD increase as the number of items stored in WM increases, reflecting the extent to which neural activity predicts the number of items stored (Erickson et al., 2019; Todd and Marois, 2005). For each participant, we calculated the slope of signal change as a function of items stored by regressing the magnitude of alpha suppression or BOLD activation onto *K* across set sizes. Note that this calculation produces negative slopes for alpha suppression and positive slopes for BOLD modulation. Figure 5 summarizes the results, averaged over the left and right hemispheres. For alpha suppression, the HCS group had a negative slope that differed significantly from zero (Z=−3.07; p<0.01) but the PSZ group did not (Z=−0.37; p=0.71). For PPC BOLD, a significant positive slope was observed in both HCS (Z=3.65; p<0.001) and PSZ (Z=2.85; p<0.01). The difference between groups that was observed in the original samples did not reach significance in the subsample as for either alpha suppression (Figure 5A; Mann-Whitney U=262.00; n_1=22; n_2=18; p=0.08) or PPC BOLD (Figure 5B; Mann-Whitney U=140.00; n_1=22; n_2=18; p=0.12).

Of central interest is the nature of the relationship between modulation of alpha suppression and PPC BOLD with increasing WM load. We therefore conducted Spearman correlations between alpha suppression and BOLD slopes to evaluate the relationship between these two indices of WM storage (see Figures 5C and 5D). We found that HCS exhibited no significant correlation between alpha suppression and BOLD slopes (r_{20}=0.14; p=0.55). By contrast, PSZ exhibited a robust correlation between these two indices (r_{16}=−0.59; p<0.01); this difference in correlation strength was statistically significant (z=2.37; p<0.05). That is, larger load-dependent modulation of alpha suppression was associated with larger load-dependent modulation of BOLD in this group. Analogous results were observed for relationships between alpha suppression and occipital BOLD slopes (see Supplement). To rule out the possibility that medication effects account for the correlation between alpha suppression and BOLD modulation, we conducted a partial correlation between these indices while covarying for participants' average CPZ dose equivalent units across the two testing sessions. We found that the correlation remained significant (r=−0.64; p<0.05). Taken together, these observations suggest that alpha suppression and posterior BOLD modulation with WM load may be constrained by a shared abnormal physiological process during WM in PSZ.

Correlations with cognition, symptoms, and medication

Table 3 lists the correlations between alpha suppression slopes, PPC BOLD slopes, and measures of symptom severity and cognitive ability for HCS and PSZ, separately. We observed a pattern of correlations within the subsample of participants that broadly resembled that of the original samples: larger negative alpha suppression slopes were significantly associated with higher performance on the WRAT-4 and WTAR cognitive measures in HCS but not PSZ; conversely, larger positive PPC BOLD slopes were significantly associated with better performance on the WASI in PSZ but not HCS. We did not observe evidence that alpha suppression slopes and PPC BOLD slopes exhibit mirrored patterns of correlations with cognitive ability across the two groups.

Discussion

We tested the hypothesis that the abnormal WM-dependent modulation of alpha suppression and PPC BOLD in PSZ are related, possibly implicating a common underlying pathological mechanism. We first examined group differences in the relationship between alpha suppression and PPC BOLD across set sizes. We found that diagnosis and set size both had a moderating effect on the relationship between PPC BOLD and alpha suppression, with PSZ exhibiting a larger negative relationship between the two indices compared to HCS. The between-groups difference in this relationship was significant at set size 4, which is likely to be the set size during which WM processes are optimally engaged. These results indicate that, among PSZ, larger BOLD signal was associated with larger alpha suppression in a set size-dependent manner as indicated by negative β weights.

We next examined the correlation between load-dependent modulation of alpha suppression and BOLD. We found that PSZ exhibited numerically shallower slopes than did HCS, although this effect did not reach statistical significance. As these effects were significant

in the original full samples, we attribute the lack of significant differences in slopes to reduced statistical power to detect such effects. Importantly, we observed a significant and robust correlation between slopes in PSZ, suggesting that the WM network dynamics that constrain alpha suppression also constrain BOLD modulation in this patient population. This robust correlation was observed even though the EEG and fMRI assessments were not performed concurrently as part of the same study; thus, this relationship is likely to be an underestimation of the true relationship between these variables.

The present results expand upon a body of literature that reveals a complex relationship between alpha power and BOLD fluctuation (e.g., Gonçalves et al., 2006). The negative relationship between alpha and BOLD that we observed in PSZ supports a model of brain function wherein alpha suppression represents a release of tonic inhibition to facilitate local processing (see Jensen and Mazaheri, 2010 for a review), which may be reflected in larger BOLD signal. However, this negative relationship was absent in HCS, indicating that this hypothesis cannot account for all observations. One possible explanation for the observed dissociation between HCS and PSZ may be between-group differences in thalamocortical connectivity. Recent modeling work has revealed that the correlation typically observed between alpha power and BOLD represents an emergent property of variation in corticothalamic and intrathalamic functional connectivity (Pang and Robinson, 2018). Together with reports that posterior thalamic nuclei exhibit hyperconnectivity with posterior cortical regions in PSZ (Anticevic et al., 2014; Cheng et al., 2015; Ramsay, 2019), it may be that between-group differences in thalamocortical connectivity can account for the inconsistent pattern of correlation between HCS and PSZ. More research is needed to directly test this intriguing hypothesis.

Finally, we did not observe a straightforward pattern of correlation between measures of cognition and these two neurophysiological indices of WM storage. In PSZ, BOLD signal but not alpha suppression slope values were correlated with IQ, while in HCS, alpha suppression but not BOLD signal slope values were correlated with tests more reflective of crystalized intellectual functioning. More research is needed to shed light on the relationship between test-based cognitive performance and alpha suppression and BOLD activation. Of note, the diverging pattern of association with test performance contradicts the possibility that the correlation between these two indices was secondary to a generalized cognitive deficit.

There are some limitations to the study. First, the analyses described here were conducted on a sub-sample of participants who completed both the Erickson et al. (2017) and Hahn et al. (2018) protocols. The relatively smaller number of participants compared to the original samples may have reduced our power to detect significant effects; furthermore, the significant effects that were observed should be replicated in a new and larger sample of participants. Second, some features of the tasks used in the two protocols were not identical, such as the length of the delay period between the sample and test arrays. We believe that these task differences are trivial given that WM capacity estimates remain stable across delay periods of 1 to 4 seconds (Gold et al., 2010). Furthermore, we observed that there was no behavioral interaction between testing session, set size, and diagnosis, suggesting that the pattern of group differences in K did not differ between the two paradigms. Finally,

future studies will be necessary to examine the specificity of the relationship between alpha suppression and BOLD modulation to the PPC and MOG regions. Altogether, the present results suggest that abnormal alpha suppression and BOLD modulation during WM storage share a common underlying neural pathology in PSZ. Future experiments exploiting the complementary strengths of fMRI and EEG techniques may pinpoint the disease mechanism underlying these cognitive deficits. (Andreasen, 1989; Hawk et al., 1975; Overall and Gorham, 1962; Wechsler, 2011, 2001; Wilkinson and Robertson, 2006)

Supplementary Material

Refer to Web version on PubMed Central for supplementary material.

Funding Source

Funding agents had no role in planning or writing of the manuscript. This work was supported by the National Institute of Mental Health Grant # R01 MH065034 to JG and SL.

References

Andreasen NC, 1989. The Scale for the Assessment of Negative Symptoms (SANS): conceptual and theoretical foundations. The British journal of psychiatry. Supplement 155, 49–58.

Andreasen NC, Pressler M, Nopoulos P, Miller D, Ho B-C, 2010. Antipsychotic dose equivalents and dose-years: a standardized method for comparing exposure to different drugs. Biological Psychiatry67, 255–262. 10.1016/j.biopsych.2009.08.040 [PubMed: 19897178]

Anticevic A, Yang G, Savic A, Murray JD, Cole MW, Repovs G, Pearlson GD, Glahn DC, 2014. Mediodorsal and Visual Thalamic Connectivity Differ in Schizophrenia and Bipolar Disorder With and Without Psychosis History. Schizophrenia Bull40, 1227–1243. 10.1093/schbul/sbu100

Bachman P, Kim J, Yee CM, Therman S, Manninen M, Lonnqvist J, Kaprio J, Huttunen MO, Naatanen R, Cannon TD, 2008. Abnormally high EEG alpha synchrony during working memory maintenance in twins discordant for schizophrenia. Schizophr Res103, 293–297. 10.1016/j.schres.2008.04.006 [PubMed: 18534822]

Cheng W, Palaniyappan L, Li M, Kendrick KM, Zhang J, Luo Q, Liu Z, Yu R, Deng W, Wang Q, Ma X, Guo W, Francis S, Liddle P, Mayer AR, Schumann G, Li T, Feng J, 2015. Voxel-based, brain-wide association study of aberrant functional connectivity in schizophrenia implicates thalamocortical circuitry. NPJ Schizophrenia1, 171–8. 10.1038/npjschz.2015.16

Cowan N, 2001. The magical number 4 in short-term memory: a reconsideration of mental storage capacity. The Behavioral and Brain Sciences24, 87–114-discussion 114-85. [PubMed: 11515286]

Cox R, 1996. AFNI: software for analysis and visualization of functional magnetic resonance neuroimages. Computational Biomedical Research29, 162–173. 10.1006/cbmr.1996.0014

Delorme A, Makeig S, 2004. EEGLAB: an open source toolbox for analysis of single-trial EEG dynamics including independent component analysis. The Journal of Neuroscience134, 9–21. 10.1016/j.jneumeth.2003.10.009

Erickson MA, Albrecht MA, Robinson B, Luck SJ, Gold JM, 2017. Impaired Suppression of Delay-Period Alpha and Beta Is Associated With Impaired Working Memory in Schizophrenia. Biological Psychiatry: Cognitive Neuroscience and Neuroimaging2, 272–279. 10.1016/j.bpsc.2016.09.003 [PubMed: 28670630]

Erickson MA, Smith D, Albrecht MA, Silverstein S, 2019. Alpha-band desynchronization reflects memory-specific processes during visual change detection. Psychophysiology56, e13442. 10.1111/psyp.13442 [PubMed: 31318065]

First MB, Spitzer RL, Gibbon M, Williams J, 2002. Clinical Interview for DSM-IV-TR Axis I Disorders, Research Version, Patient Edition (SCID-I/P). New York: New York State Psychiatric Institute.

Fukuda K, Mance I, Vogel EK, 2015. α Power Modulation and Event-Related Slow Wave Provide Dissociable Correlates of Visual Working Memory. The Journal of Neuroscience35, 14009–14016. 10.1523/jneurosci.5003-14.2015 [PubMed: 26468201]

Glahn DC, Ragland JD, Abramoff A, Barrett J, Laird AR, Bearden CE, Velligan DI, 2005. Beyond hypofrontality: A quantitative meta- analysis of functional neuroimaging studies of working memory in schizophrenia. Hum Brain Mapp25, 60–69. 10.1002/hbm.20138 [PubMed: 15846819]

Gold JM, Hahn B, Zhang WW, Robinson BM, Kappenman ES, Beck VM, Luck SJ, 2010. Reduced Capacity but Spared Precision and Maintenance of Working Memory Representations in Schizophrenia. Archives of General Psychiatry67, 570–8. 10.1001/archgenpsychiatry.2010.65 [PubMed: 20530006]

Gonçalves SI, Munck J.C. de, Pouwels PJW, Schoonhoven R, Kuijer JPA, Maurits NM, Hoogduin JM, Someren EJWV, Heethaar RM, Silva F.H.L. da, 2006. Correlating the alpha rhythm to BOLD using simultaneous EEG/fMRI: Inter-subject variability. Neuroimage30, 203–213. 10.1016/j.neuroimage.2005.09.062 [PubMed: 16290018]

Hahn B, Harvey AN, Gold JM, Ross TJ, Stein EA, 2017. Load-dependent hyperdeactivation of the default mode network in people with schizophrenia. Schizophr Res185, 190–196. 10.1016/j.schres.2017.01.001 [PubMed: 28073606]

Hahn B, Robinson BM, Leonard CJ, Luck SJ, Gold JM, 2018. Posterior Parietal Cortex Dysfunction Is Central to Working Memory Storage and Broad Cognitive Deficits in Schizophrenia. The Journal of Neuroscience38, 8378–8387. 10.1523/jneurosci.0913-18.2018 [PubMed: 30104335]

Hawk A, JR WC, Strauss J, 1975. Diagnostic Criteria and Five-Year Outcome. Archives of General Psychiatry32, 343–347. [PubMed: 1115575]

Jensen O, Mazaheri A, 2010. Shaping functional architecture by oscillatory alpha activity: gating by inhibition. Frontiers in Human Neuroscience4, 186–8. 10.3389/fnhum.2010.00186 [PubMed: 21119777]

Johnson MK, McMahon RP, Robinson BM, Harvey AN, Hahn B, Leonard CJ, Luck SJ, Gold JM, 2013. The relationship between working memory capacity and broad measures of cognitive ability in healthy adults and people with schizophrenia. Neuropsychology27, 220–229. 10.1037/a0032060 [PubMed: 23527650]

Kang SS, M. AW III, Chafee MV, Im C-H, Bernat EM, Davenport ND, Sponheim SR, 2018. Abnormal cortical neural synchrony during working memory in schizophrenia. Clinical Neurophysiology129, 210–221. 10.1016/j.clinph.2017.10.024 [PubMed: 29197736]

Kraguljac NV, Srivastava A, Lahti AC, 2013. Memory Deficits in Schizophrenia: A Selective Review of Functional Magnetic Resonance Imaging (fMRI) Studies. Behav Sci3, 330–347. 10.3390/bs3030330 [PubMed: 25379242]

Lee J, Park S, 2005. Working memory impairments in schizophrenia: a meta-analysis. Journal of Abnormal Psychology114, 599–611. 10.1037/0021-843x.114.4.599 [PubMed: 16351383]

Lopez-Calderon J, Luck SJ, 2014. ERPLAB: an open-source toolbox for the analysis of event-related potentials. Frontiers in Human Neuroscience8, 213–14. 10.3389/fnhum.2014.00213 [PubMed: 24782741]

Luck SJ, Vogel EK, 1997. The capacity of visual working memory for features and conjunctions. Nature390, 279–281. 10.1038/36846 [PubMed: 9384378]

Manoach DS, 2003. Prefrontal cortex dysfunction during working memory performance in schizophrenia: reconciling discrepant findings. Schizophr Res60, 285–298. 10.1016/s0920-9964(02)00294-3 [PubMed: 12591590]

Overall JE, Gorham DR, 1962. The Brief Psychiatric Rating Scale. Psychological Reports10, 799–812.

Pang JC, Robinson PA, 2018. Neural mechanisms of the EEG alpha-BOLD anticorrelation. Neuroimage181, 461–470. 10.1016/j.neuroimage.2018.07.031 [PubMed: 30025852]

Pashler H, 1988. Familiarity and visual change detection. Perceptual Psychophysics44, 369–378. 10.3758/bf03210419

Ramsay IS, 2019. An Activation Likelihood Estimate Meta-analysis of Thalamocortical Dysconnectivity in Psychosis. Biological Psychiatry Cognitive Neurosci Neuroimaging4, 859–869. 10.1016/j.bpsc.2019.04.007

Rouder JN, Morey RD, Morey CC, Cowan N, 2011. How to measure working memory capacity in the change detection paradigm. Psychonomic Bulletin & Review18, 324–330. 10.3758/s13423-011-0055-3 [PubMed: 21331668]

Snellenberg JXV, Torres IJ, Thornton AE, 2006. Functional Neuroimaging of Working Memory in Schizophrenia:: Task Performance as a Moderating Variable. Neuropsychology20, 497–510. 10.1037/0894-4105.20.5.497 [PubMed: 16938013]

Talairach J, Tournoux P, 1988. Co-Planar Stereotaxic Atlas of the Human Brain: 3-D Proportional System: An Approach to Cerebral Imaging. Thieme.

Todd JJ, Marois R, 2005. Posterior parietal cortex activity predicts individual differences in visual short-term memory capacity. Cognitive Affect Behav Neurosci5, 144–155. 10.3758/cabn.5.2.144

Wechsler D, 2011. WASI-II: Wechsler abbreviated scale of intelligence -- second edition, Psychological Corporation. Psychological Corporation.

Wechsler D, 2001. Wechsler Test of Adult Reading: WTAR.

Wilkinson GS, Robertson GJ, 2006. WRAT 4: Wide Range Achievement Test; professional manual.

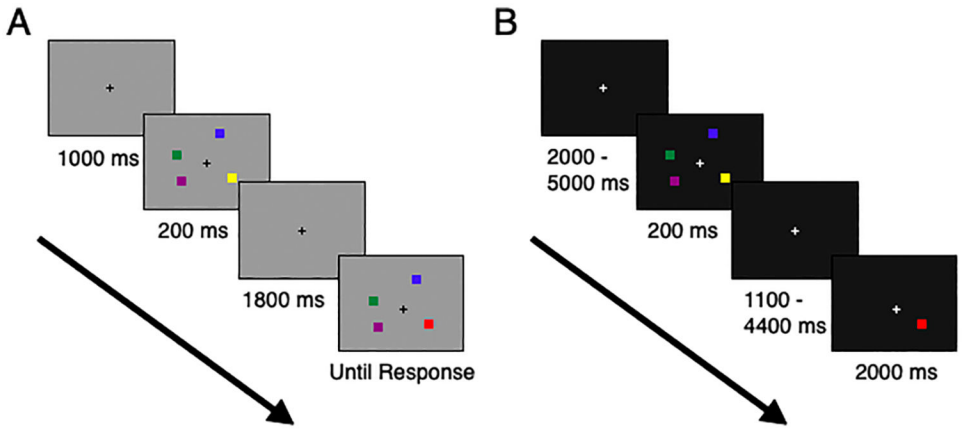

Figure 1.
Trial sequence for EEG task (A) and fMRI task (B).

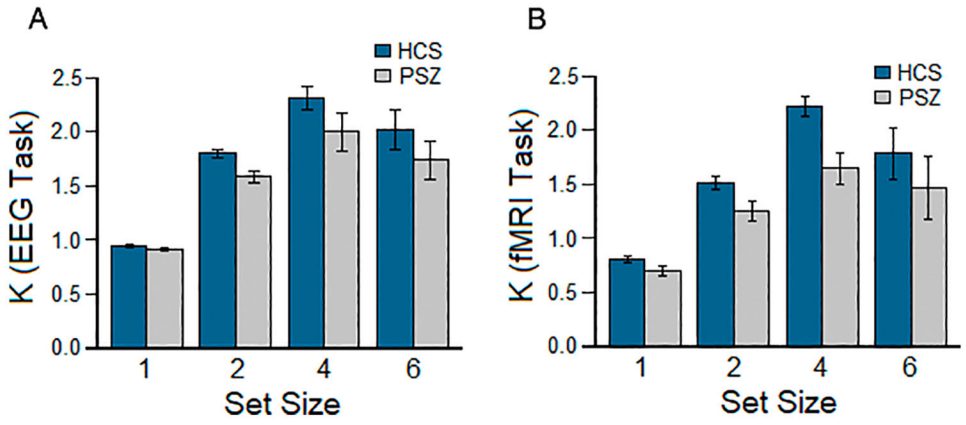

Figure 2.

Average change detection task performance for the same subsamples of HCS (N=22) and PSZ (N=18) in the EEG (A) and the fMRI session (B). There was no significant session x set size x diagnosis interaction, indicating that the pattern of group differences in performance was the same across the two testing sessions.

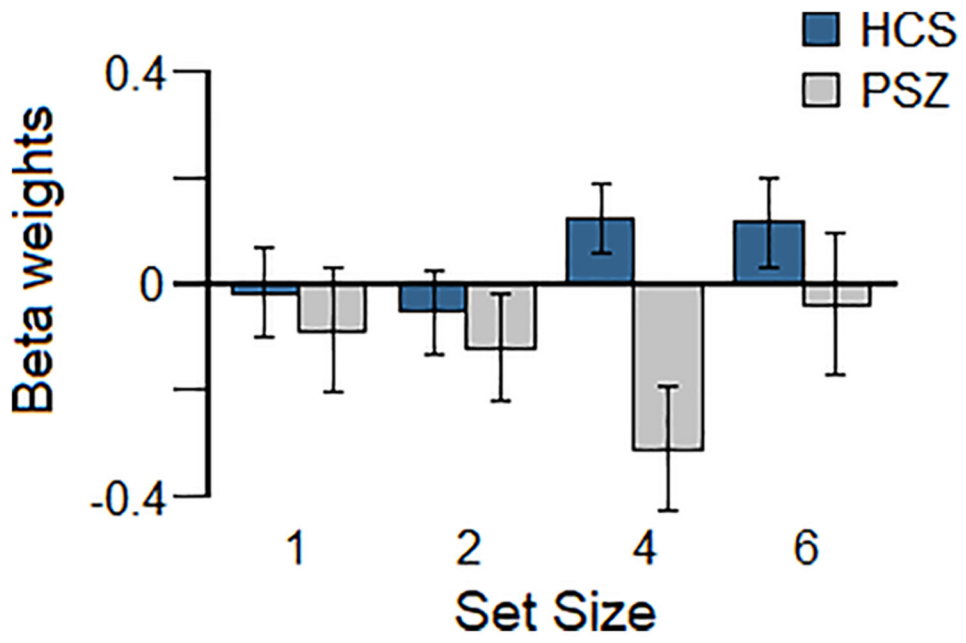

Figure 3.

Alpha suppression from the left (A) and right (B) hemisphere electrodes by set size; scalp map of alpha suppression averaged across all four set sizes (C); % BOLD signal change in the left (D) and right (E) posterior parietal cortex; posterior parietal cortex ROI's (F). HCS and PSZ both exhibited a load-dependent increase in alpha suppression and BOLD, with an interaction between set size and diagnosis.

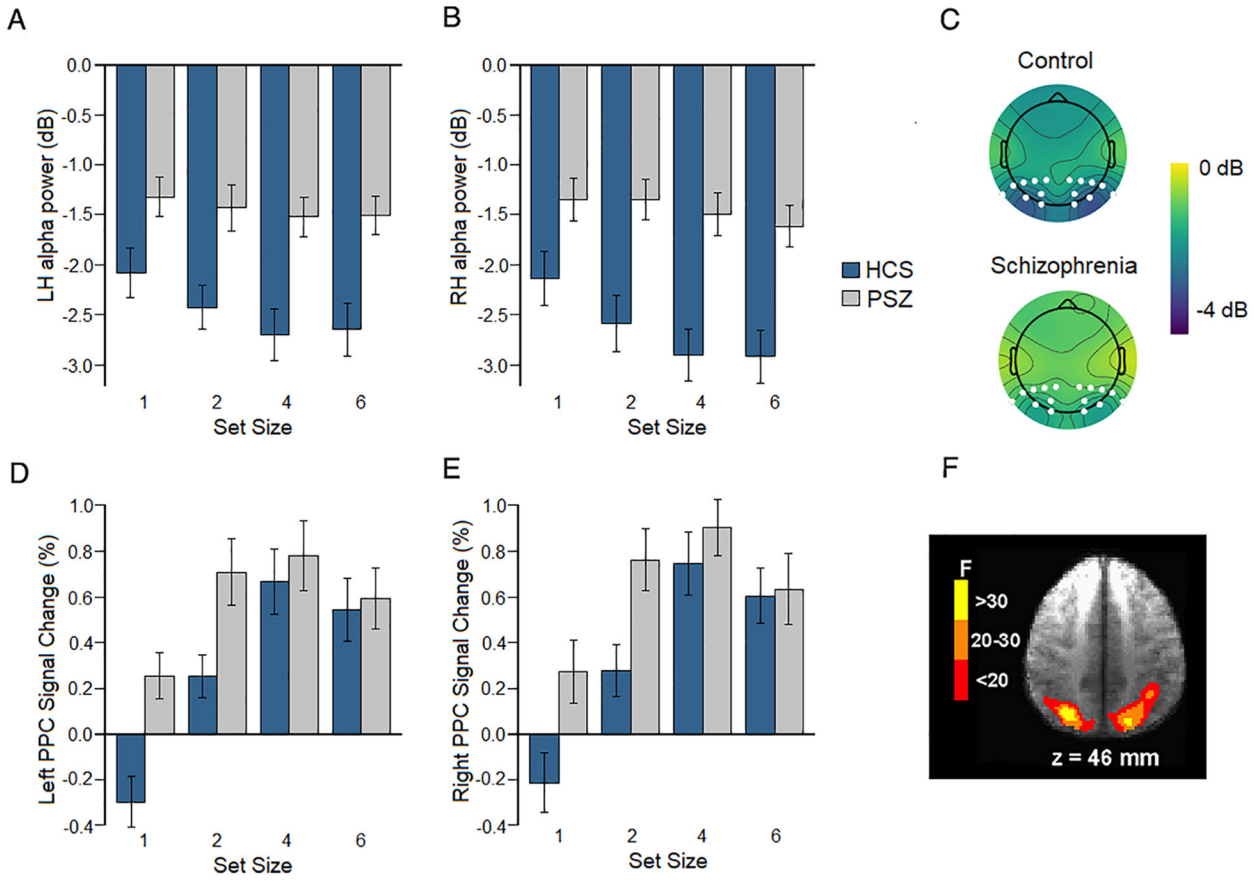

Figure 4.

Relationship between alpha suppression and BOLD at each set size by diagnostic group. PSZ exhibited more negative associations between alpha power and BOLD, with a significant group difference at set size (SS) 4.

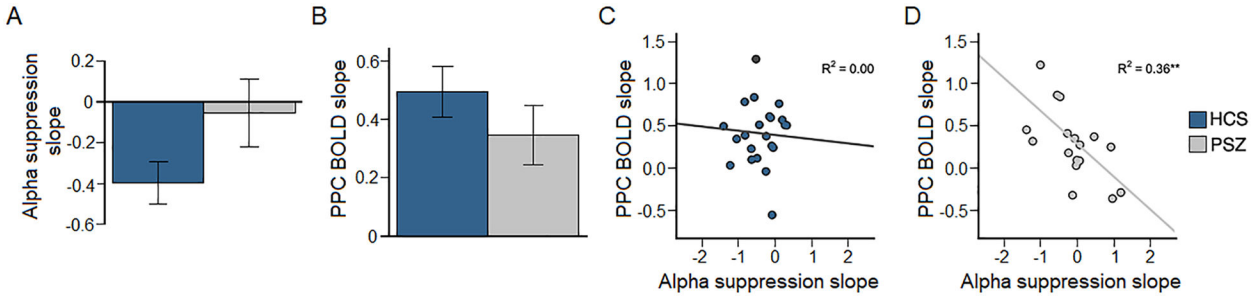

Figure 5.

Average slope following regression of alpha suppression onto K (A); average slope following regression of % BOLD signal change onto K (B); scatterplot depicting relationship between alpha suppression and BOLD slope for HCS (C) and PSZ (D). PSZ exhibited numerically but not significantly shallower slopes than did HCS, and the magnitude of those slopes was correlated among PSZ but not HCS.

$^{\Delta}p < 0.10$

**$p < 0.01$

Table 1.

Demographic information (mean ± SD)

	Healthy Controls	People with Schizophrenia
Gender (M : F)	15 : 7	13 : 5
Age		
EEG Assessment	38.05 ± 11.47	35.56 ± 10.78
fMRI Assessment	38.00 ± 11.49	36.06 ± 10.80
Race (AA : C)	8 : 14	7 : 11
Education (years)	15.50 ± 2.06	12.72 ± 2.34**
Parental Education	14.61 ± 2.46	13.75 ± 2.60
Chlorpromazine dose equivalent (mg/day)		
EEG Assessment	—	458.30 ± 326.89
fMRI Assessment	—	595.52 ± 572.32
BPRS	—	
EEG Assessment		29.72 ± 6.69
fMRI Assessment		29.56 ± 7.01
SANS	—	
EEG Assessment		22.94 ± 9.63
fMRI Assessment		21.67 ± 10.77
LOF (Total)	—	
EEG Assessment		21.89 ± 4.69
fMRI Assessment		22.22 ± 4.92
WASI	115.62 ± 6.79	104.33 ± 13.37**
WRAT-4	114.38 ± 11.88	101.94 ± 17.95*
WTAR	115.48 ± 6.47	102.39 ± 18.95*

* $p < 0.05$

** $p < 0.01$

*** $p < 0.001$

BPRS = Brief Psychiatric Rating Scale; SANS = Scale for the Assessment of Negative Symptoms; LOF = Level of Functioning; WASI = Wechsler Abbreviated Scale of Intelligence; WRAT = Wide Range Achievement Test; WTAR = Wechsler Test of Adult Reading

Table 2.

Parietal clusters identified as displaying linear activation change with working memory (K) across all 74 participants reported from Hahn et al. (2018). Occipital clusters are reported in Supplementary Table 1. The right parietal and occipital clusters were artificially separated for the purposes of the present study.

				Center of mass (mm)		
	Region	**Side**	**Volume (μL)**	**LR**	**PA**	**IS**
1	Superior & inferior parietal lobule, precuneus	R	9815	26.8	−57.9	46.8
2	Superior & inferior parietal lobule, precuneus	L	7991	46.6	−61.7	46.6

Table 3.

Correlations between alpha suppression slope, parietal BOLD slope, symptom severity, and cognition.

	HCS		PSZ	
	Alpha suppression	**Parietal BOLD**	**Alpha suppression**	**Parietal BOLD**
WASI IQ	−0.31	0.10	−0.14	0.48 *
WRAT-4	−0.54 *	0.07	0.07	0.32
WTAR	−0.47 *	0.00	0.00	0.37
Chlorpromazine Dose Equivalent	—	—	−0.09	0.21
BPRS Total	—	—	−0.14	−0.18
SANS Total	—	—	0.08	−0.32
LOF	—	—	0.32	0.44 +

+ $p < 0.10$

* $p < 0.05$

BPRS = Brief Psychiatric Rating Scale; SANS = Scale for the Assessment of Negative Symptoms; LOF = Level of Functioning; WASI = Wechsler Abbreviated Scale of Intelligence; WRAT = Wide Range Achievement Test; WTAR = Wechsler Test of Adult Reading